

## Morphometrical analysis of retinal arterial macroaneurysms

TONGALP TEZEL<sup>1</sup>, ILHAN GÜNALP<sup>2</sup> & GÜLGÜN TEZEL<sup>1</sup>

<sup>1</sup>*Clinic of Ophthalmology, Numune Hospital, Ankara;* <sup>2</sup>*Department of Ophthalmology, The Medical School of the Ankara University, Ankara, Turkey*

Accepted 23 May 1994

**Key words:** Arterial macroaneurysm, Exudate, Hemorrhage, Morphometric analysis, Retinal artery

**Abstract.** Twenty-one macroaneurysms and related vessels of 19 patients were evaluated morphometrically. Macroaneurysms were classified into two groups as hemorrhagic and exudative in terms of their major clinical sign. Average diameters of the macroaneurysms were arranged in a Gaussian distribution curve (mean and standard deviation:  $281.60 \pm 57.28$  micrometers). Regarding the distribution curve based on this data macroaneurysm can be defined as being greater than 109.76 micrometers. Macroaneurysms were most frequent on the superotemporal vessels (52.38%), followed by the inferotemporal (38.10%), inferonasal (4.76%) and superonasal vessels. Average diameter ( $r=+0.68$ ,  $p=0.0006$ ) and area ( $r=+0.71$ ,  $p=0.0003$ ) of the macroaneurysms were significantly correlated to the diameter of the relevant arterial segments. The distribution of the macroaneurysms in respect to arterial bifurcation ( $\chi^2=18.762$ ,  $p=0.0003$ ) and arteriovenous crossings ( $\chi^2=8.286$ ,  $p=0.0405$ ) were nonrandom with macroaneurysms clustering near this points. Hemorrhagic macroaneurysms were significantly closer to the optic disc ( $p<0.01$ ) and were located on relatively larger arterioles ( $p<0.01$ ). They were also more circular ( $p<0.01$ ) in shape and greater in area ( $p<0.01$ ) and diameter ( $p<0.01$ ) than the exudative ones. These findings suggest that the location of the macroaneurysm is closely related to its clinical appearance.

### Introduction

Retinal arterial macroaneurysms are acquired fusiform or asymmetric dilations of the retinal arteries that usually occur in elderly, hypertensive population. They usually develop on the first three orders of arteriolar tree [1].

Most of the macroaneurysms heals spontaneously by fibrosis, with preservation of good visual function [1, 2]. However, a few of them may cause severe visual loss by serious macular detachment, macular edema and extensive hemorrhages or exudates occupying the fovea [3, 4]. The anatomic location of a macroaneurysm with respect to fovea and disc was claimed to be a major factor in determining its clinical presentation [5]. There are also many reports about their frequent association with arterial bifurcations or arteriovenous crossings [1, 2, 5]. However no precise quantitative data about these observations has been put forward yet.

The purpose of this report is to evaluate the role of the anatomic location of a macroaneurysm in assessing its clinical appearance. This study was also undertaken to gain a more complete knowledge of the spatial distribution of macroaneurysms in respect to arterial bifurcations and arteriovenous cross-

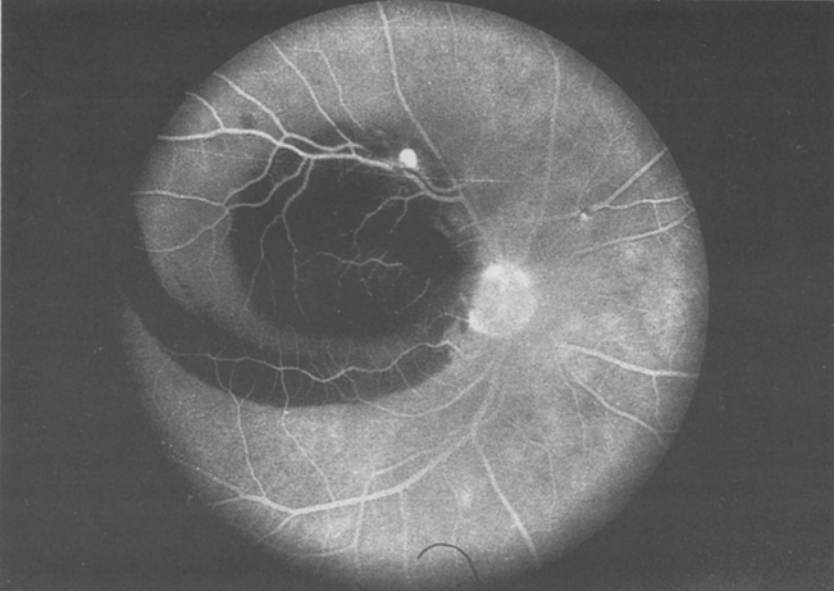


*Fig. 1.* Case 2. Fluorescein angiogram of a large circular hemorrhagic macroaneurysm on the superotemporal branch of the retinal artery. Note the borders of the macroaneurysm and the relevant vessel are clearly demonstrated.

ings. In order to put forward such relationships in absolute size units, we evaluated the color transparencies and fluorescein angiography frames of the macroaneurysms and the related vascular system morphometrically.

### **Materials and methods**

We reviewed the diagnostic records of cases with angiographically proved retinal arterial macroaneurysms who met the eligibility criteria. Criteria specific to this study included the presence of a macroaneurysm whose border and the related vessels could have been outlined appropriately to perform morphometrical analysis (Fig. 1). Four macroaneurysms of 3 patients were excluded due to partly masking by overlying retinal hemorrhage. A total of 19 patients with 21 arterial macroaneurysms were found suitable for this study.

The routine evaluation included a complete medical and ocular history, best corrected visual acuity, color fundus photographs, and fluorescein angiography. Angiography was performed in the first day the patient referred to our clinic. Macroaneurysms were divided into two groups according to their dominant clinical appearance. The 'hemorrhagic group' consisted of 12 macroaneurysms of 11 patients with hemorrhages extending more than 1 disc diameter, and were responsible for visual loss. Three of these patients

had a minor degree of associated retinal exudates, which did not have any contribution to the clinical picture. The 'exudative group' was made up of 9 macroaneurysms of 8 patients in which perianeurysmal intraretinal exudates caused by the leakage of plasma constitutes across the aneurysmal wall were the major clinical sign.

Angiograms of arterial phase were chosen for the morphometric analysis. During his early phase of the angiogram, macroaneurysm had filled with fluorescein dye but had not yet begun to leak. In later frames, fluorescein leakage obscures the border of the macroaneurysm and it became harder to delineate it. The angio frames in which the macroaneurysms were situated close to the center of frame were used to avoid the off-axis blur. This aberration is known to be varied with the object height [6] and has been reported to be negligible in the optical system of a conventional fundus camera when the image-forming bundles of a small structure such as a macroaneurysm is considered [7]. Color fundus transparencies and fluorescein angiograms of patients were projected on a chart in a scale of one to 30. To avoid distortion of the image, the projector was aligned horizontally and vertically with the center of the screen. Color transparency and fluorescein angiography frames were superimposed at least at two landmark points, that were usually the intersection of the main retinal arteries and veins. The paths of the retinal vessels were drawn on the chart. The outlines of the macroaneurysm, foveola, and optic disc were also plotted on the chart and the lengths of the following segments were measured:

- 1) Vertical and horizontal diameters of the macroaneurysm
- 2) Edge of optic nerve to the macroaneurysm
- 3) Foveola to the macroaneurysm
- 4) Diameter of the nearest visible arterial segment on which the macroaneurysm had developed

The arithmetical mean of the vertical and horizontal diameters was taken as the average diameter. The area within the outlined perimeter of the macroaneurysm was calculated by Koizumi Placom KP-80 Digital Planimeter. All the measurements were made on five separate trials by the same investigator and averaged. The circularity of the macroaneurysm was assessed by the quotient of vertical to horizontal diameter. The ocular and photographic magnification was corrected with the use of the method of Littmann [8], to obtain values in absolute size units, i.e., millimeter or square millimeter.

We performed linear regression analysis to determine whether relationships existed between:

- 1) Average diameter of the macroaneurysm and diameter of the nearest visible arterial segment

- 2) Area of the macroaneurysm and diameter of the nearest visible arterial segment.

The length of the relevant arterial segment between two successive bifurcations was divided into ten equal parts and the distribution of the macroaneurysms within these sectors was analyzed by a goodness-of-fit chi-square test. Similarly, in order to investigate the location of the macroaneurysms in respect to arteriovenous crossings the length of the arterial segment between the two successive arteriovenous crossings was also divided into ten equal zones. The distances of the macroaneurysms from the neighbouring arteriovenous crossings were expressed as the percentile of the total length of this vessel segment and their distribution within this arterial segment was analyzed by a goodness-of-fit chi-square test.

Differences in the quotient of vertical to horizontal diameter, distance from foveola, distance from disc edge, diameter of the relevant arterial segment, and the area of the macroaneurysms in exudative and hemorrhagic groups were analyzed by using Mann-Whitney U test.

Statistical analysis was performed with the computerised statistical program Microstat (Ecosoft, Inc. 1988). Probability values smaller than 0.01 were considered statistically significant.

## Results

The age of the patients ranged from 28 to 81 years, with a mean of  $63.63 \pm 15.16$  years. All the patients had unilateral involvement. Of the 19 patients reviewed 17 had a single macroaneurysm and two had double macroaneurysms. The right eye was more commonly affected (63.16%), but the difference was not statistically significant ( $\chi^2=0.842$ ,  $p=0.3588$ ). Seven of the patients (68.42%) were women. The best corrected visual acuity was ranging between light perception and 20/25. Of the 5 patients who had a visual acuity better than 20/200 three belonged to the exudative group whereas of the 14 patients with a visual acuity worse than 20/200 nine belonged to the hemorrhagic macroaneurysm group

The distribution of the macroaneurysms by quadrants was significantly nonrandom ( $\chi^2=14.62$ ,  $p=0.0007$ ) with more macroaneurysms occurring on the superotemporal vessels (52.38%), followed by the inferotemporal (38.10%), inferonasal (4.76%) and superonasal vessels (4.76%) (Fig. 2). Macroaneurysms were preferentially located on the temporal vessels ( $\chi^2=12.19$ ,  $p=0.0005$ ). No significant difference existed between the superior and inferior quadrants ( $\chi^2=0.19$ ,  $p=0.6625$ ). Macroaneurysms most often occurred in the second order of the retinal arteriolar tree (71.43%) ( $\chi^2=11.82$ ,  $p=0.0006$ ).

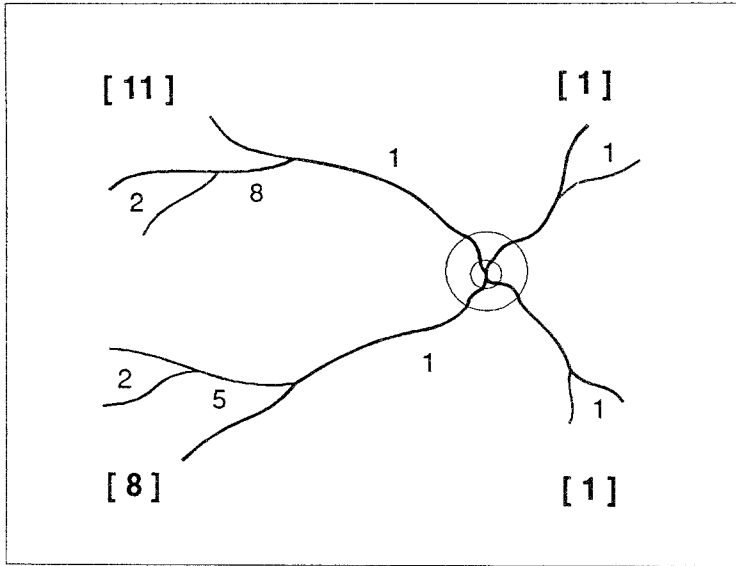


*Fig. 2.* Distribution of macroaneurysms by arterial branches. The frequency per quadrant is given in brackets.

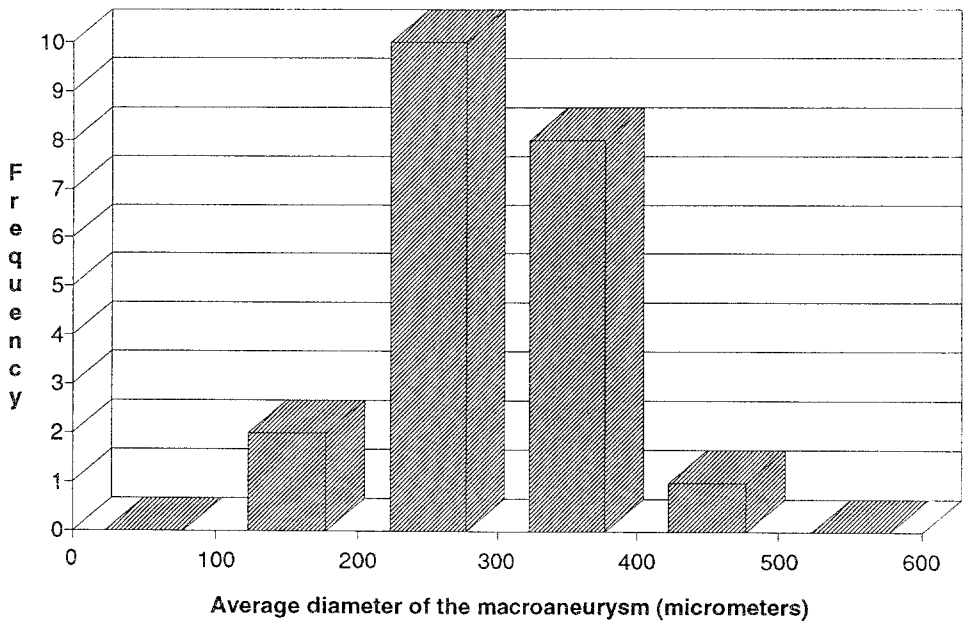


*Fig. 3.* Average diameter histogram of macroaneurysms. Mean value:  $281.60 \pm 57.28$  micrometers.

Table 1. Morphometric data

Case	Type	Vertical diameter ( $\mu$ )	Horizontal diameter ( $\mu$ )	Average diameter ( $\mu$ )	Vertical/horizontal diameter	Area ( $\mu^2$ )	Arterial diameter ( $\mu$ )	Distance to macula (mm)	Distance to disc (mm)
1	H	186.18	191.35	188.68	0.973	29100.40	103.43	2.86	2.73
2	H	424.89	438.60	431.75	0.969	166779.80	123.36	5.35	4.15
3	E	203.89	237.08	220.49	0.86	51198.70	65.80	5.06	6.68
4	H	178.18	191.89	185.04	0.929	30801.60	68.53	2.67	3.83
5	E	286.15	294.14	290.15	0.973	77818.38	95.94	4.27	5.10
6	H	342.45	356.17	349.31	0.962	101110.63	119.11	2.12	1.86
7	H	247.84	256.18	252.01	0.967	65791.32	80.61	3.64	4.44
8	E	299.40	315.18	307.29	0.95	91869.17	105.50	4.28	3.37
	E	306.40	319.13	312.78	0.96	93047.52	108.00	1.77	2.22
9	E	272.21	282.97	277.59	0.962	72056.20	89.09	7.48	8.10
10	H	306.16	316.74	311.45	0.967	82560.05	100.55	4.13	4.10
11	H	304.47	316.02	310.24	0.964	86889.85	103.62	2.74	4.77
12	E	230.55	277.43	253.99	0.831	62133.63	78.18	4.93	5.78
13	H	304.71	315.71	310.21	0.965	84327.14	101.71	3.49	3.51
14	H	280.63	288.99	284.81	0.971	75191.26	92.49	2.52	1.86
15	E	301.26	317.38	309.33	0.949	92761.58	107.30	5.30	2.76
16	H	206.87	212.04	209.46	0.976	36375.50	72.40	2.38	2.61
17	E	268.74	268.74	268.74	1	56724.96	40.31	8.83	9.41
18	H	320.11	352.11	336.11	0.909	88728.20	105.64	1.83	2.25
	H	256.09	256.09	256.09	1	51508.01	64.02	1.16	5.12
19	E	216.39	279.58	247.99	0.774	64483.79	79.89	4.21	5.03
Average		275.08	288.12	281.60	0.943	74345.60	90.74	3.86	4.27
SD		56.90	57.96	57.28	0.056	29898.24	20.67	1.90	2.01
SD=standard deviation					H=hemorrhagic type				
$\mu$ =micrometers					E=exudative type				

Regression formulas:

Average Diameter (micrometers) =  $109.62 + 1.90$  [Arterial Diameter (micrometers)]  
 $(r=+0.68, p=0.0006, F=16.7)$

Area (sq. mic.) =  $1025.58$  [Arterial Diameter (micrometers)] -  $18712.37$  ( $r=+0.71, p=0.0003, F=19.20$ )

The results of the morphometric analysis are given in Table 1. Average diameter of the macroaneurysms ranged from 185.04 to 431.75 micrometers (mean and standard deviation:  $281.60 \pm 57.28$  micrometers). The distribution of the average diameter of the macroaneurysms was not different from a Gaussian distribution curve at 95% confidence level ( $\chi^2=7.571, p=0.1815$ ) (Fig 3).

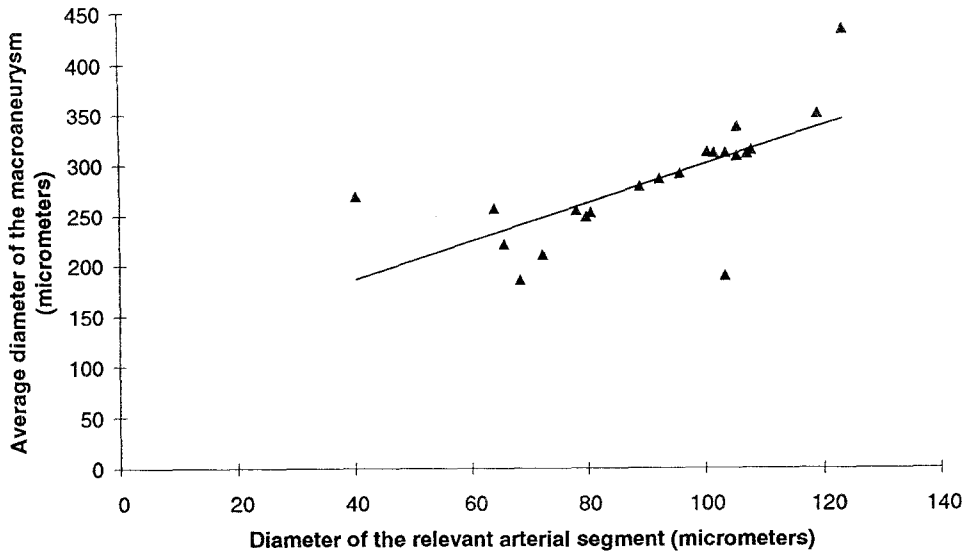


Fig. 4. Scattergram of average diameter correlated with relevant arterial diameter in 21 retinal arterial macroaneurysms. Correlation coefficient = +0.68, slope of the regression line = 1.90,  $p = 0.0006$ .

Average diameter of the macroaneurysm was significantly correlated to the diameter of the relevant arterial segments ( $r=+0.68$ ,  $p=0.0006$ ) (Table 1) (Fig. 4). Similarly, the area of the macroaneurysms developed on larger arterioles were greater than the ones that developed on relatively smaller vessels ( $r=+0.71$ ,  $p=0.0003$ ) (Table 1) (Fig. 5).

Locations of the macroaneurysms within the standardized distance of two successive arterial bifurcations are seen in Fig. 6. The distribution of the macroaneurysms in respect to arterial bifurcations was nonrandom with a clear trend toward the macroaneurysms being found near the arterial bifurcations ( $\chi^2=18.762$ ,  $p=0.0003$ ). Of the 21 macroaneurysms 11 (52.38%) were clustered on the 1/10<sup>th</sup> of the distance between the two successive arterial bifurcations.

The distribution of macroaneurysms by arteriovenous crossings was also significantly nonrandom ( $\chi^2=8.286$ ,  $p=0.0405$ ) with a clustering of macroaneurysms near arteriovenous crossing points. Of the 21 macroaneurysms 9 (42.86%) were gathered on the 1/10th of the distance between the two consecutive arteriovenous crossings (Fig. 7).

Differences between the hemorrhagic and exudative macroaneurysms concerning the average quotient of vertical to horizontal diameter ( $p<0.01$ ), area ( $p<0.01$ ), average diameter ( $p<0.01$ ), vertical diameter ( $p<0.01$ ) and horizontal diameter ( $p<0.01$ ) of the macroaneurysm were significant (Table 2).

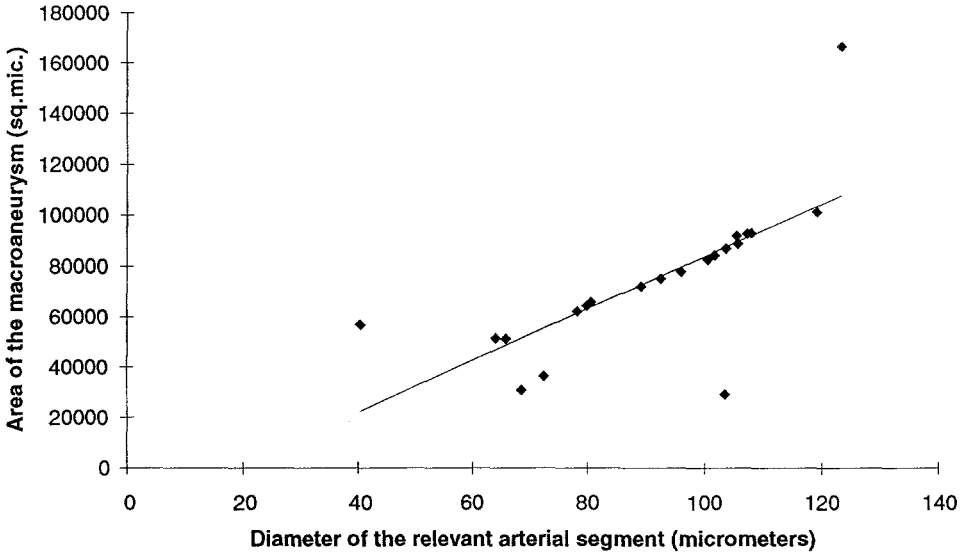


Fig. 5. Scattergram of area correlated with relevant arterial diameter in 21 retinal arterial macroaneurysms. Correlation coefficient = +0.71, slope of the regression line = 1.86,  $p=0.0006$ .

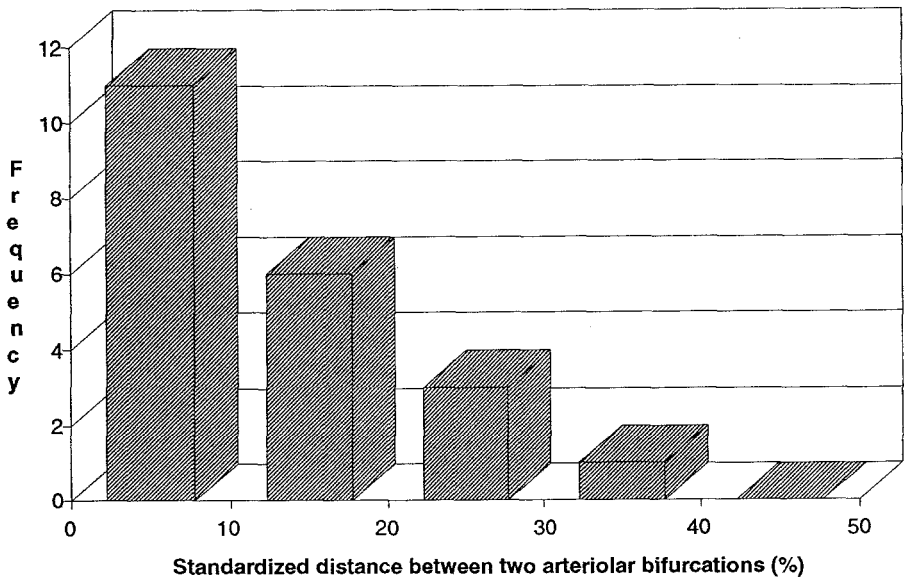
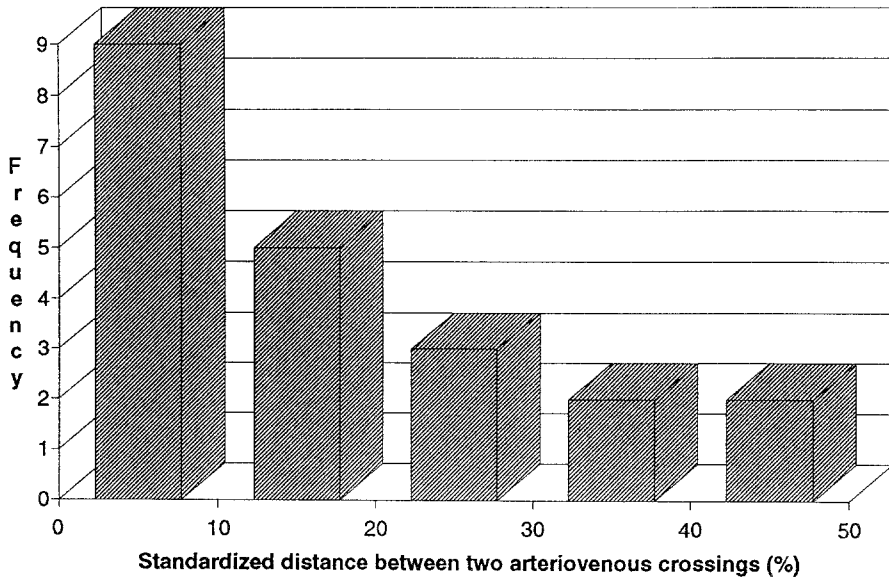


Fig. 6. Distribution of macroaneurysms on the arterial segment between two successive arterial bifurcations. The location of the macroaneurysm to the nearest bifurcation is standardized as a quotient of the total length between the bifurcations. Macroaneurysms were significantly clustered near the bifurcations ( $p=0.0003$ ).





*Fig. 7.* Distribution of macroaneurysms on the arterial segment between two successive arteriovenous crossings. The location of the macroaneurysm to the nearest arteriovenous crossing is standardized as a quotient of the total length between the arteriovenous crossings. There was a clear trend toward the macroaneurysms being found near the arteriovenous crossings ( $p=0.04$ ).

Hemorrhagic macroaneurysms were significantly more circular and greater and than the exudative ones. They were located significantly closer to the optic disc ( $p<0.01$ ) as compared with exudative macroaneurysms. No significant differences were detected between two groups in the distance to foveola ( $p>0.01$ ). The difference in the diameter of the relevant arterioles between two groups was also significant ( $p<0.01$ ), suggesting that the hemorrhagic macroaneurysms develop on relatively greater arterial segments.

## Discussion

This study was undertaken to determine whether the spatial characteristics of the macroaneurysms are related to their clinical presentation, and can give hints about their pathogenesis.

The average diameters of the macroaneurysms were arranged in a Gaussian distribution curve with a mean value of  $281,60 \pm 57.28$  micrometers. The aneurysms at the lower end of this size spectrum can be defined as microaneurysms. Their size is expected to exceed the limits set by the mean value minus three standard deviations. Only, 0.13% of all macroaneurysms fall outside of this mark according to the Gaussian distribution curve. Thus obtained

Table 2. Comparison of the morphometric data

	Hemorrhagic type	Exudative type	p*
Quotient of vertical to horizontal diameter	0.963 ± 0.023	0.918 ± 0.077	< 0.01
Distance from fovea to macroaneurysm (mm)	2.91 ± 1.12	5.13 ± 2.03	> 0.01
Distance from disc to macroaneurysm (mm)	3.44 ± 1.14	5.38 ± 2.41	< 0.01
Area ( $\mu^2$ )	74930.31 ± 37861.05	73565.99 ± 16203.67	< 0.01
Average diameter of the macroaneurysm ( $\mu$ )	285.43 ± 72.08	276.48 ± 31.71	< 0.01
Vertical diameter of the macroaneurysm ( $\mu$ )	282.13 ± 69.71	265 ± 38.75	< 0.01
Horizontal diameter of the macroaneurysm ( $\mu$ )	290.99 ± 73.91	287.96 ± 26.88	< 0.01
Diameter of the artery ( $\mu$ )	94.62 ± 19.31	85.56 ± 22.41	< 0.01

\* Mann-Whitney U test;  $\mu$ = micrometers

average diameter of 109,76 micrometers was close to 100 micrometers that was previously defined as the upper limit of microaneurysms [9].

Macroaneurysm formation is often ascribed to the mechanical effects of the intraluminal arterial pressure [1, 5]. We found that both the average diameter and the area of the macroaneurysm were highly correlated with the relevant arteriolar diameter. This correlation confirms the effect of the intraluminal pressure on the morphology of the macroaneurysm. Blood flow and thus the transmural stress, increases exponentially along with the increase of the arterial diameter [10]. As a result the closer the macroaneurysm is to the disc, the more pressure will be applied on its wall, and the greater would be its dimension. However, during their evolutionary phases, macroaneurysms can rest still on different stages for various periods [11].

Using morphometric image analysis we determined that nearly half of the macroaneurysms were located within one tenth of the distance of the arterial segment between the two adjacent arterial bifurcations or arteriovenous crossings. The nonrandom distribution of macroaneurysms near arteriovenous crossings and arterial bifurcations in our study can be attributed to the disturbance of the normal non-Newtonian blood flow at these points. The turbulent blood flow at arteriovenous crossings and bifurcations may increase the possibility of endothelial damage [12] and may constitute an initial step

in the evolution of the macroaneurysms [13]. On the other hand, at arteriovenous crossings both vessels share a common adventitial and glial sheath. The arterial wall has less structural support at this point and may be apt to dilate easily resulting in an aneurysm. Moreover, various pathologies of the adjacent venule may disturb the integrity of the artery wall leading to the aneurysmal dilatation [5, 13].

Of the 21 macroaneurysms 19 were located on the temporal vessels. The greater transmural tension due to three times greater blood flow in these vessels may explain the frequent occurrence of macroaneurysms on temporal vessels [10]. This marked preference for the superotemporal vessels may also be related to the greater number of arteriovenous crossings in this quadrant [14]. It should also be kept in mind that macroaneurysms at this site may often cause macular edema and hemorrhages, with the consequent loss of vision that brings the patient to the ophthalmologist more frequently.

Of the 21 macroaneurysms 15 were sited within the second order of arteriolar bifurcations. The arterial segments within this zone are located close to the optic disc and have relatively high transmural pressures [10]. Furthermore, the second order of the retinal arterial tree may be more prone to develop macroaneurysms due to a more tortuous course, numerous subdivisions and the greater number of arteriovenous crossings [14–16].

Our findings suggest that the mechanical effect due to intraluminal pressure also play a major role in determining the clinical features of the macroaneurysm. Hemorrhagic macroaneurysms were located significantly closer to the disc and on relatively wider vessel segments where the flow rates and intraluminal pressures were high. High intraluminal pressure at these segments can easily overcome the counter resistance of the arterial wall tension at all points resulting in round saccular macroaneurysms. This would explain why the hemorrhagic macroaneurysms had significantly higher quotient of vertical to horizontal diameter than those with exudative macroaneurysms. The exudative type of macroaneurysms on the other hand were generally located on the arteriolar segments that were far away from the disc. In these vessel segments pressure is not high enough to rupture the wall, but it can disturb the permeability of it, causing the leakage of serum into the surrounding retina. Furthermore, the relatively low intraluminal pressure in these vessel segments, can not overcome the arterial wall tension at all points easily. The most damaged portion, with the least intrinsic resistance will dilate readily but, the magnitude of the net force leading to aneurysmal dilatation will gradually decrease by approaching the partially undamaged wall segments. The resultant aneurysm will have a fusiform appearance, as is shown by the low the quotient of vertical to horizontal diameter.

Relationship between the location of the macroaneurysm and its clinical presentation has been reported previously but to our knowledge no quantitative data has been put forward [2, 3, 5, 17]. Our findings suggest that whatever the causes of arterial aneurysm formation the intraluminal pressure and the strength of the compromised vessel wall determine the final appearance and the clinical presentation of the macroaneurysm. Macroaneurysms that develop on the vessels close to the optic disc enlarge uniformly under a greater transmural stress and prone to bleed. Macroaneurysms started on the peripheral vessels are not under such a great stress. However the arteriolar wall of peripheral vessels is relatively weak. As a result the damaged portion of the vessel wall will dilate outwards and attain a smaller, fusiform appearance. The low pressure will not disturb the integrity of the aneurysmal wall but plasma constituents will leak out.

In conclusion, these observations show that hemorrhagic or exudative evolution of macroaneurysms could be predicted with some accuracy using the morphometrical findings. Since the prognosis and therapeutic approaches may differ for exudative and hemorrhagic macroaneurysms the ability to detect the morphometrical features may promote the development of more effective therapeutic methods.

## References

1. Robertson DM. Macroaneurysms of the retinal arteries. *Ophthalmology* (Rochester) 1973; 77: 55-67.
2. Badii G, Messmer EP. Spontanregression bei erworbenem arteriellen Makroaneurysma der Retina. *Klin Mbl Augenheilk* 1992; 200: 537-8.
3. Abdel-Khalek MN, Richardson J. Retinal Macroaneurysm: natural history and guidelines for treatment. *Br J Ophthalmol* 1986; 70: 2-11.
4. Noble KG. Retinal macroaneurysms. *Ophthalmology* 1984; 91:108-9.
5. Lavin MJ, Marsh RJ, Peart S, Rehman A. Retinal macroaneurysms: a retrospective study of 40 patients. *Br J Ophthalmol* 1987; 71: 817-25.
6. O'Shea D. Elements of modern optical design. New York: John Wiley and Sons, 1987: 192.
7. Pomerantzeff O, Webb RH, Delori FC. Image formation in fundus cameras. *Invest Ophthalmol Vis Sci* 1979; 18: 630-7.
8. Littmann H. Zur Bestimmung der wahren Grösse eines Objektes auf dem Hintergrund des lebenden Auges. *Klin Mbl Augenheilk* 1988; 192: 66-7.
9. Wise G, Dollery C, Henkind P. The retinal circulation. New York: Harper & Row, 1971: 278-84.
10. Feke GT, Tagawa H, Deupree DM, Goger DG, Sebag L, Weiter JJ. Blood flow in normal human retina. *Invest Ophthalmol Vis Sci* 1989; 30: 58-65.
11. Iwasawa A, Majima A, Shirai S, Taki M. Bilateral prepapillary macroaneurysm. Report of a case. *Jap J Clin Ophthal* 1989; 43: 619-23.
12. Perktold K, Peter R, Resch M. Pulsatile non-newtonian blood flow simulation through a bifurcation with an aneurysm. *Biorheology* 1989; 26: 1011-30.
13. Fichte C, Streeten BW, Friedman AH. A histopathologic study retinal arterial aneurysms. *Am J Ophthalmol* 1978; 85: 509-18.

14. Weinberg DV, Egan KM, Seddon JM. Asymmetric distribution of arteriovenous crossings in the normal retina. *Ophthalmology* 1993; 100: 31–36.
15. Schröder S, Schmid-Schönbein GW, Schmid-Schönbein H, Brab M, Reim M. Methode zur Erfassung der Netzwerktopologie der menschlichen Retinagesasse. *Klin Mbl Augenheilk* 1990; 197: 33–39.
16. Mainster MA. The fractal properties of retinal vessels: embryological and clinical implications. *Eye* 1990; 4: 235–241.
17. Palestine AG, Robertson DM, Goldstein BG. Macroaneurysms of the retinal arteries. *Am J Ophthalmol* 1982; 93: 164–71.

*Address for correspondence:* Tongalp H. Tezel, Şerefli sokak 36/6, Mebusevleri, Tandoğan, 06580 Ankara, Turkey  
Phone: (90-4) 2213064